Since January 2020 Elsevier has created a COVID-19 resource centre with free information in English and Mandarin on the novel coronavirus COVID-19. The COVID-19 resource centre is hosted on Elsevier Connect, the company's public news and information website.

Elsevier hereby grants permission to make all its COVID-19-related research that is available on the COVID-19 resource centre - including this research content - immediately available in PubMed Central and other publicly funded repositories, such as the WHO COVID database with rights for unrestricted research re-use and analyses in any form or by any means with acknowledgement of the original source. These permissions are granted for free by Elsevier for as long as the COVID-19 resource centre remains active.

CHAPTER

11

Rhinovirus RNA Polymerase: Structure, Function, and Inhibitors

Sonam Nirwan and Rita Kakkar

Department of Chemistry, University of Delhi, Delhi, India

11.1 INTRODUCTION

Human rhinoviruses (HRVs), first discovered in the 1950s, are responsible for more than one-half of cold-like illnesses (Pitkaranta and Hayden, 1998). Other viral pathogens associated with the common cold are the coronaviruses, respiratory syncytial virus (RSV), influenza virus, parainfluenza virus, and adenovirus (Monto and Cavallaro, 1971). Prematurely born infants and older children with asthma are particularly at risk of developing severe rhinovirus (RV) infections. RVs enter via the upper respiratory tract and bind to respiratory epithelial cells via several receptors, which are different, depending on the RV species. However, while once thought to cause relatively not so harmful upper respiratory tract illness, HRVs are now linked to increase in the severity of chronic pulmonary disease, asthma development (Kim and Gern, 2012) and, more recently, severe bronchiolitis in infants and children, as well as fatal pneumonia in elderly and immune compromised adults.

RVs are nonenveloped viruses with a single-stranded positive-sense RNA genome of approximately 7200 nt of the genus *Enterovirus* in the family *Picornaviridae*. Their genomes have a long highly structured 51 nontranslated regions (NTRs), a single large open reading frame (ORF) and a short 31 NTR, terminated with a poly (A) tail. In the cytoplasm of the host cell, the ORF is first translated into a polyprotein, which is then processed by viral proteases to release the structural proteins (VP1-4), and the nonstructural proteins (2A−2B−2C−3A−3B−3Cpro−$3D^{pol}$ and

DOI: https://doi.org/10.1016/B978-0-12-815422-9.00011-5

© 2019 Elsevier Inc. All rights reserved.

in some genera L) as well as some stable precursors necessary for virus replication in host cells (Paul, 2002). Out of these nonstructural proteins, a key component of the replication machinery of the picornavirus family is the RNA-dependent RNA polymerase (RdRP), also referred to as 3D polymerase ($3D^{pol}$).

The RdRP (also known as $3D^{pol}$) belongs to a superfamily of template directed nucleic acid polymerases, including DNA-dependent DNA polymerases (DdDPs), DNA-dependent RNA polymerases (DdRPs), and reverse transcriptases (RTs). All these enzymes share a cupped right-hand structure (including fingers, palm, and thumb domains). RdRPs exist in unique "closed-hand" conformation, in contrast to the "open-hand" found in other polynucleotide polymerases. This closed conformation comprises several motifs (A−D) that are the conserved features of particular RdRPs and performs different roles in the catalytic activity of the enzyme. Crystal structures of three serotypes (HRV1B, HRV14, and HRV16) have been reported (Love et al., 2004). These crystal structures provide deep insights about the structural arrangement and the conformational dynamic changes associated with the enzyme.

Using positive-sense RNA template, the enzyme synthesizes daughter minus RNA strand using a primer-dependent mechanism. The primer utilized in the mechanism is the uridylylated form of VPg protein. The process of uridylyation of Vpg is also performed by $3D^{pol}$. Based on this positive-sense RNA template, the correct NTP molecule is added to the 8−9 nucleotide long primer resulting in the growing double-stranded daughter strand. Three well-defined channels have been identified in the RdRP structures, serving as the entry paths for template (template channel) and for nucleoside triphosphates (nucleoside triphosphate channel), respectively, and the exit path for the double-stranded RNA product (central channel). It performs the function of catalyzing phosphodiester bond formation through a conserved two-metal ion mechanism, wherein the two metal ions are present in the active site of the enzyme (Steitz, 1998).

Together with other viral and host proteins, this enzyme performs its function of replicating the RV RNA genome in the cytoplasm of host cells. As this class of polymerases is unique to RNA viruses and has no host counterpart, the viral RdRP represents a very attractive target for antiviral design. This biochemical activity is not present in mammalian cells; thus, very selective inhibitors could be designed that target only the virus without producing side effects. However, owing to the existence of more than 100 serotypes and variability at the antigenic site, efforts made at vaccine development are hindered. To date, specific drugs that prevent or reduce RV infection are not available. Thus, this opens a wide avenue to design novel "anti-rhinoviral" drugs.

11.2 CLASSIFICATION

HRV is classified into three genetically distinct groups: HRV-A (containing 74 serotypes), HRV-B (containing 25 serotypes), and HRV-C. HRV-C is a novel group discovered by the International Committee on Taxonomy of Viruses in 2009 (Lamson et al., 2006). Another classification is based on the nature of the receptor group utilized by the polymerase enzyme in infecting the host cell. Out of 100 distinct serotypes of RVs identified, 90% of these utilize ICAM-1 (intercellular adhesion molecules) as a receptor for infecting HeLa cells and are thus referred to as the "*major*" *receptor group* (Tomassini and Colonno, 1986; Greve et al., 1989). All the remaining RV serotypes, with one exception, utilize the LDL (low-density lipoprotein) receptor (Hofer et al., 1994) and are referred to as the "*minor*" *receptor group.* A systematic evaluation of a group of capsid-binding agents (15 compounds) against all serotyped HRV revealed the existence of two antiviral groups, A and B, based upon differential susceptibility to these antiviral compounds. HRV14 and poliovirus (PV) belong to group A, while HRV16 and HRVIA belong to group B (Andries et al., 1990).

11.3 STRUCTURAL FEATURES OF HRV POLYMERASE

11.3.1 Crystal Structure of HRV $3D^{pol}$

The crystal structures for the three main serotypes (HRV1B, HRV16, and HRV14) of the enzyme were solved by Love and his group. All the three crystal structures superimposed closely, but the largest difference arose in the external residues and this could arise from crystal packing as well as sequence variation (Love et al., 2004).

HRV $3D^{pol}$ displays the typical "right-hand" arrangement of fingers, palm, and thumb domains and its folding topology resembles that of RdRPs from hepatitis C virus (HCV) (Ago et al., 1999; Lesburg et al., 1999) and rabbit hemorrhagic disease virus (RHDV) (Ng et al., 2002). Also, HRV $3D^{pol}$ resembles most closely to PV $3D^{pol}$ enzyme (Hansen et al., 1997), except at the N terminus. Excluding PV residues 12–25, superposition of the two gives a root mean square deviation (rmsd) of 1.14 Å for HRV14 (64% identity), 1.18 Å for HRV16 (56% identity), and 1.12 Å for HRV1B (57% identity), and that is why PV RdRP is sometimes considered while studying inhibitors for HRV RdRP. The complete view offered by HRV $3D^{pol}$ confirms a conservation of tertiary structure among RdRPs from diverse RNA viruses and that is why RdRPs is a very promising target for developing multitarget antiviral drugs having broad range of biological activity. Differences observed in

the secondary structure of these polymerases reflect not only the substrate diversity but also divergent mechanisms for initiation of RNA synthesis (primer dependent for HRV and RHDV but primer independent for HCV and bacteriophage φ6). Three well-defined channels have been identified in the RdRP structures that allow access to the active site of the incoming ribonucleoside triphosphate (rNTPs) and the RNA template, as well as the exit path of the newly synthesized daughter-strand RNA (dsRNA) product (Ferrer-Orta et al., 2006).

11.3.2 Description of Individual Domains

According to the crystal structure of serotype HRV1B solved by Love and his coworkers, the *finger domain* can be divided into an N-terminal segment containing the first 54 residues, an "inner" region surrounding the palm domain, and an "outer" region projecting away from the palm. The N-terminal segment folds back on itself, forming a smaller loop (residues 41–53), which sits at the top of the polymerase molecule and forms contacts with the tip of the fingers subdomain. This N-terminal segment serves as a bridge reaching across to form interactions with the thumb domain. This bridging of the fingers and thumb subdomains is unique to RdRPs and gives them a globular shape rather than the U shape observed in the DNA polymerases, DdRPs, and the HIV RT. It could be possible that the disruption in the N-terminal region leads to the inactivity of the polymerase.

The "inner fingers" region consists primarily of helices α3, α9, α10, α13, and α14 which surround round and pack against the palm domain. The "outer fingers" region includes: (1) a five stranded β sheet (β1, β6, β8, β10, and β11), (2) an adjacent helix α4 and β-hairpin β4–β5, and (3) a loop formed by β7 and α8. Strand β8 containing motif F (residues 172–176) is unique to the RdRP family (Ago et al., 1999). This motif F contains residue Arg174, which is a highly conserved residue of HRV, and interacts with the α-phosphate of the nascent NTP (Huang et al., 1998). A topological feature of HRV $3D^{pol}$ which is unique to picornaviral RdRPs is the β-hairpin defined by β4–β5 (residues 102–104 and 107–109). Differences are observed in the serotype HRV16 $3D^{pol}$, as compared to HRV1B, where a unique small loop (residues 102–108) is inserted after a short α-helix on the front face of the finger subdomain and motif F comprises residues 167–176.

The *palm subdomain* (residues 201–242 and 291–373) is defined by the central β-sheet β9, β12, and β13 surrounded by helices α11, α15, and α16. Often referred to as the catalytic subdomain, the palm subdomain is rich in conserved structural motifs, motifs A–E. Motif A (residues 229–241) is defined by β9 and α12 and contains an important conserved

residue Asp234, one of the primary magnesium coordination residues required for catalysis. Motif A also contains Asp239, which plays a key role in discriminating between ribonuleotides and 2′-deoxyribonucleotides by hydrogen bonding to the 2′-OH of NTP (Hansen et al., 1997). Motif B (residues 291−308) includes most of the helix α15, along with highly conserved Asn296, which forms hydrogen bonds to Asp239 and positions the latter for NTP recognition (Hansen et al., 1997). Motif C (residues 319−334) contains Asp327, which, along with Asp234, are absolutely required for the nucleotidyl transfer reaction and are responsible for chelation of two magnesium ions at the active site. Motif D provides structural support to motif A. An additional conserved structural element unique to RNA-dependent polymerases is motif E (residues 368−377) that forms a tight loop which lies at the junction between the palm and thumb subdomains. The turn of this loop projects into the active site cavity where it helps to position the 3′ end of the primer strand in proper orientation for the attack on the α-phosphate of the NTP during phosphoryl transfer (Jacobo-Molina et al., 1993). Similar structural features of the palm domain with motifs A−E are observed for the other serotypes of HRV.

The *thumb subdomain* of HRV $3D^{Pol}$ (serotype HRV1B) is formed by four long helices α17, α18, α19, α21, and the short helix α20, all of which superimpose well with PV $3D^{Pol}$. The folding topology of the HVR1B thumb is similar to the RHDV enzyme, except that the latter lacks the short helix α20. Structural differences are observed for HRV16 $3D^{Pol}$ compared to HRV1B, since it consists of three antiparallel α-helices followed by an extended loop segment which connects to an additional C terminal α-helix. The thumb subdomain of HRV16 $3D^{Pol}$ differs considerably from that of HCV, BVDV, and φ6 polymerases also. The larger thumb subdomain of HCV NS5B contains more than twice the number of residues as compared to HRV16 $3Dp^{ol}$ and includes three additional α-helices and a β-loop structure. Unlike HCV, where the C-terminal helix fills the active site, the C-terminal helix of HRV16 $3D^{Pol}$ packs against the front faces of the molecule in such a way to leave the active site cavity largely exposed (Appleby et al., 2005).

11.3.3 Potassium Binding Site

During crystallographic refinement of HRV1B $3D^{Pol}$, a potential monovalent cation (potassium-binding site) was identified at the interface between the inner and outer fingers domain. The local geometry of this site is found to be preserved in HRV14 and HRV16 $3D^{Pol}$. HRV1B crystallization scheme employs high concentrations of potassium and sodium. It has been observed experimentally that the enzyme's

polymerase activity is higher in assay buffer containing potassium ions relative to sodium ions. Furthermore, at low concentrations, potassium has a modest stimulatory effect on HRV $3D^{pol}$ polymerase activity (Hung et al., 2002).

The proposed potassium-binding site in HRV $3D^{pol}$ is about 15 Å from the catalytic residues and does not appear to be directly involved in the polymerase activity or RNA binding. Potassium ion more likely plays a structural role by stabilizing one end of the finger's domain β-sheet which includes the N terminus). This site is also adjacent to conserved motifs A and B and thus facilitates their positional stability (Love et al., 2004). The potassium-binding site cannot be predicted properly for PV $3D^{pol}$ since this site is present in the disordered region of the enzyme.

11.3.4 Metal Binding at the Active Site

Conserved aspartic acid residues in the polymerase palm domains coordinate the two magnesium ions needed for the catalytic polymerization reaction of the enzyme, with one metal activating the primer 3′ OH for the attack of the nucleotide α-phosphate, and the other metal serving to stabilize the triphosphate moiety (Fig. 11.1). Since it is not possible to obtain HRV $3D^{pol}$ crystals with the bound divalent cation (Mg^{2+}) and NTP, HRV14 $3D^{pol}$ is cocrystallized with trivalent Sm^{3+}, where Sm^{3+} is found to occupy a position similar to divalent Mg^{2+}. There occurs coordination by Asp327 and Asp328 from motif C and Asp234 from motif A.

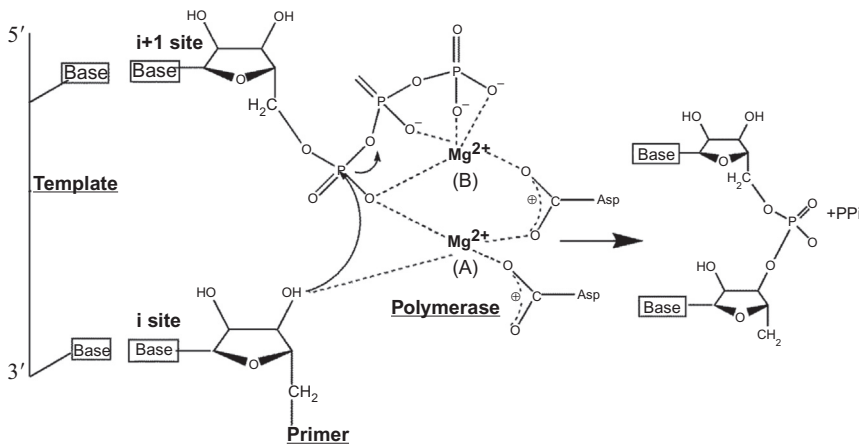

FIGURE 11.1 A diagram showing two-metal mechanism used by polymerases to catalyze the nucleotidyl transfer reaction. Source: *Reprinted with permission from Choi, K.H., 2012. Viral polymerases. In: Viral Molecular Machines. Springer, Boston, MA, pp. 267–304. Copyright 2017 Springer Nature.*

An additional electrostatic interaction is found in HRV14 $3D^{pol}$ between the bound Sm^{3+} and Asp357 (distance ~4.9 Å). Comparison of HRV14 $3D^{pol}$ structures obtained with and without Sm^{3+}, and comparison of HRV/Sm^{3+} to unbound HRV16 or HRV1B serotypes, shows that the binding of the metal causes a shift of the strand β-9 (containing Asp234) and a parallel strand β-14 (containing Asp357) inward toward the metal (Love et al., 2004). However, no global conformational change was observed upon binding of a metal at the active site, consistent with the findings from the several HCV NS5B structures containing bound metals and NTP (Ago et al., 1999).

Mg^{2+} in the active site plays another role of ensuring substrate specificity apart from its role in the catalytic transfer of the nucleotidyl moiety to the growing RNA strand. In the presence of Mg^{2+}, the enzyme displays strong base and sugar specificity and follows the primer-dependent activity. However, when Mg^{2+} was replaced by Mn^{2+}, the specificity for ribonucleotides was lost, utilization of deoxnucleotides became possible and primer-independent de novo activity was observed on the poly (C) template (Hung et al., 2002). The primer-independent synthesis on a heteropolymeric hairpin RNA was performed using a copy-back mechanism previously reported for HCV NS5B (Behrens et al., 1996). The optimum Mg^{2+} concentration needed for the activity of HRV16 3D polymerase was 1.5 mM which is comparable to the 3 mM required for the activity of PV and EMCV 3D polymerases.

It is interesting to note that unlike in HRV16 serotype, in case of HRV2 $3D^{pol}$, it is Mn^{2+} that catalyzes both VPg uridylylation and VPg-poly (U) synthesis on a poly (A) template by about 100-fold over those in the presence of Mg^{2+}. Whether or not the stimulatory activity of Mn^{2+} is due to an enhanced binding of the enzyme to the poly (A)-VPg complex is not yet known (Gerber et al., 2001).

11.3.5 Modeling of Duplex Oligonucleotide for HRV $3D^{pol}$

The enzyme uses the positive-sense RNA template to add the correct NTP molecule to the growing daughter strand. This occurs in the active site where the template and the initial short nucleotide chain known as primer interact to form a duplex. In the HRV $3D^{pol}$ duplex mode there are three domains; each of these plays a significant role in supporting this primer-template duplex by interacting with the sugar phosphate backbone. It consists of the palm domain, finger domain, and the thumb domain. HRV residues 18−22 and 130−138, which show relatively high mobility in the crystal structure, are located near the expected "entry" of the template strand (5′ end) and "exit" of the primer strand (5′ end), respectively. Asp239 is positioned to form a hydrogen bond with the

2′ OH group of NTP, which is responsible for the ribonucleotide discrimination within the RdRP family. Arg174 interacts with the triphosphate moiety of NTP. β-hairpin β4−β5 interacts with the major groove of the duplex, possibly serving as a "guide" analogous to the role proposed for the β-loop of HCV NS5B. In the absence of direct structural evidence relating to how these physiological substrates bind in the exposed active site of HRV16 $3D^{Pol}$, actually the HIV RT ternary complex structure (Huang et al., 1998), was used as a guide to model this template−primer duplex and an incoming rNTP molecule in the active site.

11.3.6 Potential Oligomerization Interfaces

Oligomerization of protein refers to the interaction of more than one polypeptide chains. This forms the quaternary structure, generally considered to be the highest level of organization within the protein structural hierarchy. Oligomeric proteins may be composed either exclusively of several copies of identical polypeptide chains, in which case they are termed homo-oligomers, or alternatively by at least one copy of different polypeptide chains (hetero-oligomers).

RdRPs can oligomerize through reversible associations mediated by electrostatic and hydrophobic interactions, hydrogen bonds or by covalent stabilization by disulfide bonds. Oligomerization is predominantly observed in vitro during crystallization, probably due to the high protein concentration, as well as by other factors like pH or ionic strength of the solution. Intracellular accumulation of oligomeric polymerases was observed during viral infection of different RNA viruses, including PV, Sendai virus, Rift Valley Fever virus, and norovirus, among others. Within the crystal lattice of PV $3D^{Pol}$, molecules interact through two extensive contact surfaces referred to as interfaces I and interfaces II (Hansen et al., 1997), giving rise to higher order structures that have been proposed to explain the oligomerization (Beckman and Kirkegaard, 1998). Disruption of contacts forming interfaces I in PV $3D^{Pol}$ crystals diminishes biochemically detected oligomerization. Of the three serotypes of HRVs (HRV14, 16, 1B) none forms crystal lattice contacts resembling interfaces II of PV. Furthermore, neither HRV16 nor HRV1B $3D^{Pol}$ show interactions found in interfaces I of PV. However, HRV14 $3D^{Pol}$ contains an intermolecular contact similar to the interface I. However, the two salt bridges forming interface I in PV are not present in HRV14. It is important to note that the oligomerization phenomenon has not been reported till now for any HRV serotypes. Also, there is no current evidence which shows that oligomerization plays any role in HRV functioning

(Pathak et al., 2002), but the study of the oligomerization phenomena in HRV polymerase can help in understanding the protein evolution and higher order complexity associated with it.

11.3.7 Conformational Analysis Showing the Flexibility of the Enzyme

Conformational analysis of protein structure is advantageous as it gives an idea about the flexible and restricted regions of the protein. This flexibility of protein is essential for protein function and the dynamics of these regions can be modulated by allosteric effectors, either activating or inhibiting the biological activity of the protein.

An important conformational property of all viral RdRPs is their "closed-hand" conformation, as opposed to the "open hand" or U shaped observed in other polynucleotide polymerases. Here in case of HRV $3D^{Pol}$, this closed conformation is accomplished by interconnecting the fingers and thumb domains through the N-terminal portion of the protein and through several loops protruding from the fingers, named the fingertips, which completely encircle the active site of the enzyme. The closed-hand conformation stabilizes a relatively rigid unit. However, different structural data showed that the thumb domain can rotate a few degrees, relative to the fingers and palm, giving a more open conformation that is found to be the inactive form of the enzyme (Ng et al., 2002). The recent structure of HCV genotype 2a RdRP revealed an extreme case of this "open" conformation, in which the contact between the fingertips and thumb is partially disrupted (Biswal et al., 2005). Molecular dynamics simulations were performed by the Cameron laboratory on the various picornaviral polymerases including PV, HRV, Coxsackievirus B3 (CVB3), and foot-and-mouth disease virus (FMDV) (Moustafa et al., 2011) and the results showed conserved patterns of flexibility. molecular dynamics (MD) studies showed that the largest flexibility was located at the fingers domain, whereas the lowest flexibility was concentrated in the palm. The conserved structural motifs involved in primer, template, and/or nucleotide binding (motifs A, D–F) were all quite flexible, even those located in the palm domain. In contrast, the structural motifs whose primary role is to serve as ligands to the divalent cations required for nucleotidyl transfer (the portion of motif A harboring AspA, the α-helix of motif B containing AsnB and motif C) appeared to be much less flexible. All these dynamic elements could be modulated by external effectors, which appear to be effective allosteric inhibitors that could block or disturb the flexibility of these enzymes,

ultimately reducing their catalytic function. Among all structural movements observed, motif B and the β-loop at its N-terminus in particular, came out to be the new potential druggable targets (Garriga et al., 2013).

11.3.8 Role of Motif D as Fidelity Checkpoint

The role of RdRP is critical, not only for the virus life cycle, but also for its adaptive potential. The combination of low fidelity of replication and the absence of proofreading and excision activities within the RdRPs result in high mutation frequencies that allow these viruses a rapid adaptation to changing environments. Data obtained revealed that the palm mutations produced the greatest effects on the in vitro nucleotide discrimination. This makes these virus species "quasi-species" where individual members of the virus population have some distribution of point mutations relative to a consensus sequence. Limiting the quasi-species variation with a high fidelity polymerase variant could prevent the spread of the virus within a mouse model (Pfeiffer and Kirkegaard, 2005). Interestingly, reduction in the fidelity can limit the virus growth, as shown by recent Coxsackie virus studies, wherein low fidelity polymerase variants resulted in viruses that replicated well in tissue culture, but then rapidly extinguished and failed to establish persistent infections in animal models (Gnadig et al., 2012).

Kinetic studies have suggested that the nucleotidyl transfer chemical step and a conformational change in step 2 (Fig. 11.2) played an important role in the fidelity checkpoints. Motif D plays a unique role in this conformational step and helps in limiting the misincorporation of nucleotide (Arnold et al., 2005).

Many polymerases use conformational dynamics of a conserved alpha helix to permit correct nucleotide addition. This alpha helix is missing in structures of RdRPs and RTs. Conserved motif D and specifically the residue lysine in this motif plays the substitute role of the alpha helix in other RdRPs. Motif D plays an important role in nucleotide addition and

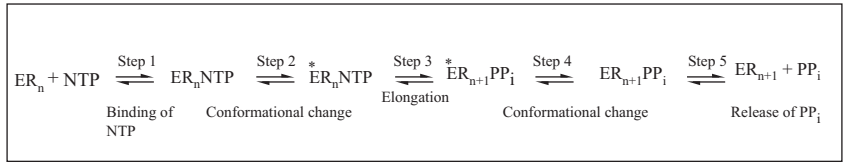

FIGURE 11.2 A diagram showing RNA-dependent RNA polymerase (RdRP) kinetic mechanism that includes a prechemistry conformational rearrangement (step 2) required for catalytic competence of the RdRP–RNA–NTP complex in the forward (nucleotide incorporation) direction. Step 2 is where the conformational changes in motif D occurs.

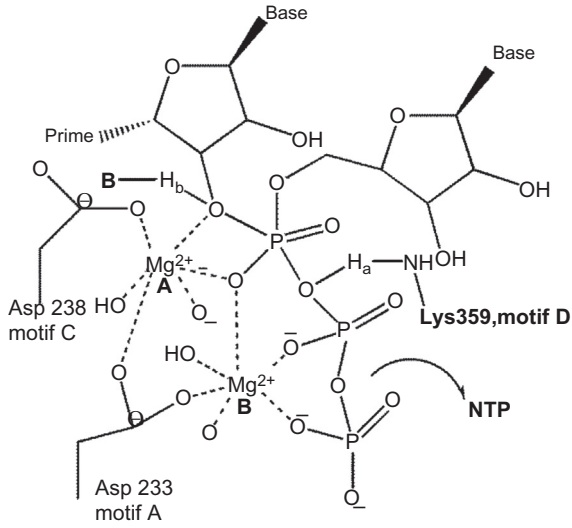

FIGURE 11.3 A diagram showing proton transfer reaction. As the transition state of nucleotidyl transfer is approached, the 3′-OH proton (H_b) of primer terminus is abstracted by an unidentified base (B) and the pyrophosphate leaving group of nucleoside triphosphate is protonated (H_a) by the lysine general acid.

maintaining the fidelity. The lysine residue acts as a general acid, it protonates the leaving pyrophosphate group during the nucleotidyl transfer reaction. This proton transfer reaction, as shown in Fig. 11.3, while not essential to catalysis, is found to enhance the rate of nucleotidyl transfer by 50- to 2000-fold (Castro et al., 2007, 2009). Mutation of the motif D lysine leads to a dramatic decrease in the nucleotidyl transfer rate and increases the fidelity of the polymerase reaction, hence controlling the diverse population of the virus (Vignuzzi et al., 2008).

Yang and coworkers performed the solution state NMR titration studies for PV to show how motif D acts as a checkpoint by differentiating the binding of correct vs. incorrect nucleotide, thus maintaining the fidelity of the enzyme. Motif D is a conserved structural feature in PV and RV RdRPs. Hence, the result obtained for PV could be extended to RV. In particular, binding of the correct nucleotide produces a large chemical shift change to residue Met354 in accordance with a conformational change in motif D, whereas incorrect nucleotide binding fails to produce such a large chemical shift with respect to residue Met354, suggesting that closed conformation of the enzyme is not reached when the incorrect nucleotide binds. Thus, binding of the incorrect nucleotide appears to perturb the position of motif D and shift the conformational equilibrium away from the closed conformation, which is essential for the active state, i.e., it shifts the equilibrium to the left in step 2 of the

kinetic mechanism (Fig. 11.2) and hence acts as a parameter in the fidelity checkpoint (Yang et al., 2012).

11.4 BIOCHEMICAL CHARACTERIZATION OF $3D^{pol}$

11.4.1 Optimization of the HRV16 Polymerase Reaction Conditions

The reaction conditions for the HRV16 3D-6His polymerase were optimized using poly (A) as the template and biotinylated oligo (dU) 15 as the primer in NEN Flash Plates (Hung et al., 2002). The incubation temperature was varied between 12 and 37°C, and the optimum temperature was found to be approximately 30°C. At temperatures between 32 and 37°C, there was a dramatic decrease in activity. Using the optimum temperature of 30°C, the pH dependence of RdRP activity displayed a bell-shaped curve with the optimum pH of 7.3. Divalent metal ions were absolutely required for activity and the optimum concentration for Mg^{2+} was 1 mM. Mn^{2+} was able to substitute for Mg^{2+} while stimulating the activity by 2.5-fold at the optimum concentration of 1 mM. However, the polymerase activity dropped sharply at 3 mM Mn^{2+}. KCl added at low concentrations (<10 mM) indicate that the monovalent cation K^+ exhibits a modest stimulatory effect but becomes inhibitory at higher concentrations, with the optimum activity observed at 10 mM.

11.4.2 HRV16 3D Polymerase Activity on Homopolymeric and Heteropolymeric Templates

HRV16 3D polymerase shows varying preferences for different homopolymeric RNA templates. It efficiently acts on poly (A) and poly (C) templates while exhibiting no activity on poly (G) and poly (U) templates. While the polymerase activity of HRV16 $3D^{Pol}$ is primer-dependent for all four homopolymeric templates in the presence of Mg^{2+}, primer-independent de novo RNA synthesis or terminal transferase activity was observed on poly (C) alone when Mg^{2+} was replaced with Mn^{2+}. This phenomenon was previously observed with PV 3D polymerase (Arnold and Cameron, 1999), whereas for heteropolymeric hairpin RNA, HRV16 $3D^{Pol}$ was capable of showing primer-independent synthesis using a copy-back mechanism previously reported for HCV NS5B (Behrens et al., 1996), thus producing a dimer.

11.4.3 Kinetic Analysis of HRV16 Polymerase

The Michaelis–Menten constant (K_m) and the catalytic constant (k_{cat}) values determined for UTP (uridine-5′-triphosphate) as substrate using

poly (A) as template were within fourfold of the corresponding parameters previously described for PV 3D polymerase (Arnold and Cameron, 1999). The higher efficiency of the poly (A) template as compared with poly (C) was mainly shown in the turnover rate of the nucleotide substrate where the k_{cat} for UTP was about 11-fold greater than the k_{cat} for GTP (guanosine-5′-triphosphate). GTP is a purine nucleoside triphosphate, whereas UTP is a pyrimidine nucleoside triphosphate, both acting as substrates during RNA synthesis. This further suggests that the polymerase enzyme may be more processive on the poly (A) template compared with the poly (C) template. On the other hand, the K_m for GTP is 17-fold lower than that of UTP, suggesting that the number of hydrogen bonds involved in base pairing with the complementary nucleotide on the template may also contribute to efficient binding of the nucleotide substrate to the polymerase complex, where GTP can form three hydrogen bonds whereas UTP forms only two hydrogen bonds.

11.4.4 Substrate Specificity of HRV16 3D polymerase

We studied the substrate specificity for HRV16 3D polymerase in the presence of either 1.5 mM Mg^{2+} or Mn^{2+} by testing the ability of the enzyme to incorporate different nucleotides into nucleic acid products. In the presence of Mg^{2+}, HRV16 3D was accurate in the utilization of only NTPs complementary to the template and had no RT activity. In the presence of Mg^{2+}, the enzyme could not polymerize dTMP (deoxythymidine monophosphate), suggesting that the enzyme was devoid of significant RT activity. Unlike PV 3D polymerase, replacement of Mg^{2+} by Mn^{2+} did not affect the base specificity of HRV16 3D, but severely compromised the ability of the enzyme to discriminate the sugar moiety of the nucleotide substrates. When Mg^{2+} was replaced by Mn^{2+}, sugar specificity was compromised, RT activity was stimulated by 800-fold and misincorporation of dTMP during active RNA polymerization was increased by 1200-fold.

11.5 FUNCTIONS OF HRV POLYMERASE

The HRV genome encodes an RdRP designated as 3D polymerase ($3D^{Pol}$) which is required for (1) replication of the HRV RNA genome and also (2) catalyzes the covalent linkage of UMP to a tyrosine residue on a short peptide encoded by 3B (denoted as VPg) which works as the primer in the replication process. Therefore, HRV 3D polymerase possesses two distinct enzymatic functions.

11.5.1 RNA Replication

The main function of the polymerase is to copy a template nucleic acid strand to produce a daughter strand. Hence, the primary catalytic activity of a polymerase is to transfer a nucleotidyl moiety of an incoming nucleoside triphosphate (NTP) that is complementary to the template strand to the 3′-OH end of a growing daughter strand of RNA or DNA. The polymerase active site thus must have binding sites for a template strand, the DNA or RNA primer terminus (the initiation "i" site), and the incoming NTP (the "i + 1" site).

The catalytic reaction consists of the following steps: (**1**) binding of template–primer and NTP, (**2**) incorporation of nucleoside monophosphate into the growing daughter strand, (**3**) release of pyrophosphate, and (**4**) translocation along the template. The binding of the template–primer–NTP complex is modeled based on HIV RT ternary complex structure (Huang et al., 1998), as depicted in the modeling of the duplex in the above section. The second step of nucleotidyl transfer to the growing daughter strand is performed with the help of two divalent metal ions in the active site. Both the metal ions would stabilize the charge and geometry of the pentavalent transition state during the nucleotidyl transfer reaction (Fig. 11.1). In the third step, the 3′-OH of the RNA or DNA primer terminus attacks the α-phosphate of the NTP, and a new phosphodiester bond is formed with a release of pyrophosphate. Upon release of a pyrophosphate product, in the fourth step, the newly formed RNA or DNA primer terminus translocates by one base from the site i + 1 to the site i, and this nucleotidyl transfer process is repeated until the whole template strand is copied or a termination signal appears. The reaction steps of the whole catalytic activity can be broadly divided into three steps: initiation, elongation, and termination.

11.5.1.1 Initiation

Unlike cellular DNA and RNA polymerases, which require oligonucleotides to initiate nucleic acid synthesis, viral polymerases can initiate genome replication using a variety of mechanisms reflecting their adaptation to the host cell. All known polymerases synthesize nucleic acid in the 5′ to 3′ direction and thus initiate the nucleotidyl transfer reaction at the 3′ end of the template strand. Polymerases use one of two initiation mechanisms, either a primer-dependent or a de novo (primer-independent) mechanism.

Primer-dependent initiation mechanism can be performed in four ways (Fig. 11.4). It may require (1) *Oligonucleotide priming:* A short leader RNA (two to five nucleotides) synthesized by viral RdRPs during abortive cycling that can act as primer. (2) *Cap-snatching:* Oligonucleotides cleaved from the 5′ end of a capped cellular mRNA

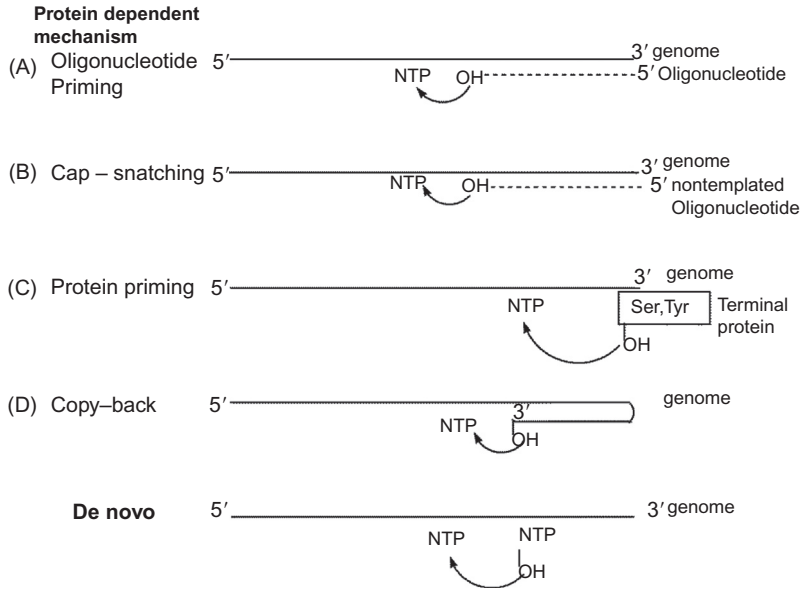

FIGURE 11.4 Schematic diagram of two initiation mechanisms used by viral polymerases. Primer-dependent mechanism: the primers can be (A) an oligonucleotide, (B) a snatched cap from host mRNA, (C) a terminal protein, or (D) the 3′ terminus of the template strand that folds back onto itself. De novo initiation mechanism: requires no short polypeptide but only another NTP molecule. Source: *Reprinted with permission from Choi, K.H., 2012. Viral polymerases. In: Viral Molecular Machines. Springer, Boston, MA, pp. 267–304. Copyright 2017 Springer Nature.*

are being used by many segmented negative-strand RNA viruses for transcription. (3) *Protein priming:* With protein-primed initiation, an amino acid provides the hydroxyl group for the formation of a phosphodiester bond with the first nucleotide. This mechanism is used by the family *Picornaviridae* (Xiang et al., 1997) as well as DNA viruses such as adenoviruses and bacteriophages w29 and PRD1. RV RNA polymerase performs its initiation step using this mechanism only. The amino acid used by the enzyme is Tyrosine. (4) *Copy back:* With template primed initiation (also known as loop-back, copy-back, turn-around, or back-priming synthesis), the 3′ end of the template RNA loops back on itself to serve as a primer.

Discussing the de novo initiation, also known as primer-independent initiation, requires interactions of at least the following four components: (1) the RdRP, (2) the RNA template with a virus-specific initiation nucleotide, (3) the initiation nucleoside triphosphate (D1), and (4) a second NTP (D2). The first phosphodiester bond is formed between D1 and D2. The initiation nucleotide (essentially a one-nucleotide primer)

provides the 3′-OH for the addition of the next nucleotide. De novo RNA synthesis is advantageous over the primer dependent one, since no genetic information is lost during replication and no additional enzymes are needed to generate the primer or to cleave the region between the template and the newly synthesized daughter RNA. In most cases, the productive de novo initiation event is immediately followed by elongation. However, in some instances, de novo initiation leads to the formation of abortive RNA products (abortive initiation) or gives rise to short RNA oligonucleotides that are subsequently used as primers (known as prime and realign mechanism).

Polymerases from *Picornaviridae* that use a primer to initiate nucleotide synthesis have small thumb domains and thus have wider template-binding channels necessary to accommodate both a template and a primer, unlike polymerases that use de novo initiation, which have large thumb domains and thus have narrower template-binding channels that can accommodate only single-stranded RNA and NTPs. RV RdRP follows a primer-dependent mechanism. Under this, it follows a *protein−primer* pathway. It utilizes the uridylylated form of VPg protein as its primer. The process of uridylyation of Vpg is also performed by $3D^{Pol}$.

De novo initiation of viral RNA (vRNA) synthesis seems to involve a higher K_m for D1 than for other NTPs indicating that initiation is the replication efficiency-limiting step that may be subject to additional regulation. Initiation efficiency can be affected by the affinity of the polymerase for the initiation nucleotide of the template (T1) and the initiation NTPs (D1 and D2). For instance, biochemical analysis shows that for BVDV RdRP, the N3- and C4-amino groups of the initiation template cytidylate are essential for RNA synthesis (Kim et al., 2000). Consistently, GTP is the preferred D1 nucleotide for RdRPs of BMV (Quadt et al., 1993), Qb (Yoshinari et al., 2000), BVDV, HCV, GB virus C (GBV-C), and members of the family *Cystoviridae*.

Temperature also plays an important role in deciding whether RdRP follows the primer dependent or primer independent mechanism. For example, the recombinant dengue virus RdRP can either initiate RNA polymerization using de novo or by extending the template 3′ terminus by back priming. At moderate temperatures, the enzyme predominantly uses de novo initiation, whereas back priming dominates at elevated temperatures (Ackermann and Padmanabhan, 2001). Based on these results and the observed structural differences between the PV and HCV RdRP, a steric model for dengue RdRP was suggested, where it can exist in either a closed or an open conformation, wherein the open one is favored at higher temperatures. The open conformation binds to a fold-back structure at the 3′ terminus of the template with the subsequent elongation producing a dimerized product. Conversely, the

closed conformation, favored at lower temperatures, recognizes the single-stranded 3′ terminus of the template and initiates de novo synthesis. Such a temperature dependence has not been studied in case of HRV yet, but possible conformation changes on temperature change can lead to such an observed behavior.

In an attempt to gain more insights into RV RNA replication, Morrow and group studied RdRP from HeLa cells infected with human rhinovirus type 2 (HRV-2). They found that a partially purified preparation of RV RNA polymerase copies vRNA without an added primer, whereas a more purified preparation is completely inactive in copying vRNA unless it is provided with a HeLa cell protein (host factor) or a synthetic oligouridylic acid [oligo(U)] primer. This suggests that the host cell protein (or host factor) is essential for the initiation step of RV RNA replication (Morrow et al., 1985).

11.5.1.2 Elongation

The elongation process of RNA replication is divided into three steps: nucleotide selection, phosphodiester bond formation, and translocation to the next nucleotide of the template for the next round of nucleotide addition. The structures of Coxsackievirus, RV, and PV polymerases elongation complexes (ECs) are solved by Engineering RNA-Mediated Crystal Contacts (Gong et al., 2013). The following points can be inferred regarding EC of RV (HRV16) and the structural similarities that are conserved among all three types.

11.5.1.2.1 RNA Interactions in the Active Site

The EC of PV polymerase provided a required view about how the template and the RNA strand interact as they thread through the active site and showed that viral RdRPs use a unique palm-based structural change to close their active site for catalysis (Gong and Peersen, 2010). A comparison of available RdRP structures further showed that this palm-based mechanism is likely to be used by all the positive-strand RNA virus polymerases (including RV) and the authors hypothesized that it evolved because the fingers domains of these polymerases made a key structural contact with the top of the thumb domain that tethered the fingers, precluding swinging motions.

Within the active site, the templating +1 nucleotide is always found fully stacked on the upstream RNA duplex and prepositioned for hydrogen-bonding interactions with the incoming NTP. The next templating nucleotide, i.e., at the +2 position in the downstream direction, is found above the active site where its base moiety is bound in a pocket formed between Pro20 and Lys22 from the index finger. At the product side of the active site strong electron density can be observed for a conserved and noncanonical A-form backbone orientation

of the phosphodiester linkage between the −1 and −2 nucleotides of the template strand. This conformation is due to buried salt bridges between Lys127 and the −1 phosphate and between Arg188 and the −2 phosphate, and together these interactions hold the 2′ ribose unit in tight contact with the conserved RdRP motif B located at the junction of the palm and fingers domains.

In particular, two residues within motif B of PV, Ser, and Asn (Asn296 in HRV), and an Asp residue (Asp239 in HRV) at the C-terminus of motif A, strictly conserved among picornavirus and caliciviruses, form the ribose-binding pocket. These amino acids interact with the ribose hydroxyl groups of the incoming rNTP, thus help in the stabilization of the subtle positioning of the palm domain that results in the conformation favoring the functional active site. An incorrect nucleotide can also bind, but its ribose hydroxyl will not be correctly positioned by these residues for the active site closure; and in consequence of this the incorporation efficiency of incorrect nucleotide will be reduced.

11.5.1.2.2 Two Proton Transfer Mechanism in the Transition State for Nucleotidyl Transfer and Formation of Phosphodiester Bond

Proton-inventory experiments performed by Castro and group showed that two protons are being transferred during the rate-limiting transition state of the reaction, suggesting that both deprotonation of the 3′-hydroxyl nucleophile (H_a) and protonation of the pyrophosphate leaving group (H_b) occur in the transition state for phosphodiester bond formation (Fig. 11.5). These data suggest the existence of a general base

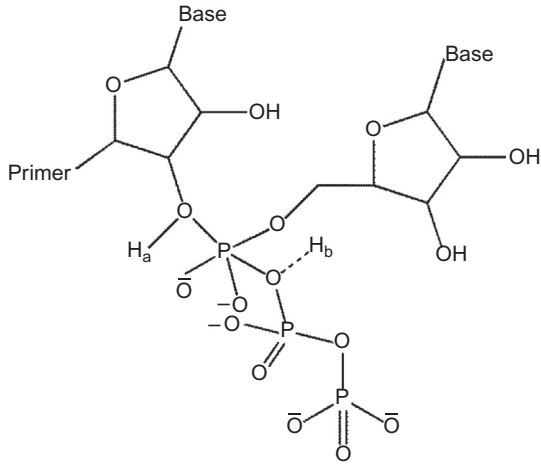

FIGURE 11.5 A diagram showing two proton transfer mechanism involved in the nucleotidyl transfer process.

for deprotonation of the 3′-OH nucleophile, although use of a water molecule cannot be ruled out conclusively, and a general acid for protonation of the pyrophosphate leaving group (which happens to be a Lysine residue) in all nucleic acid polymerases (Castro et al., 2007).

11.5.1.2.3 Downstream and Upstream Template RNA Interactions

It is known that all polymerases synthesize the RNA strand in the 5′ to 3′ end. For that, they attack the 3′ OH group of the template. Thus, the upstream position is the 5′ end of the RNA strand and the 3′ end of template, whereas the downstream position will be the 3′ end of RNA and the 5′ end of the template. Discussing the downstream and upstream positions in the EC of polymerase enzyme can help in visualizing how the template strand and the complimentary RNA strand interact and occupy the space in the enzyme going from 5′ (upstream) to 3′ (downstream) direction of the RNA transcription.

Crystal packing contacts stabilize the orientation of the downstream RNA stem-loop in the RV EC. The polymerase index finger and pinky finger regions form the cleft on which the downstream RNA duplex rides as thick noodles. The RV EC is the only structure where we observe significant contacts involving the downstream template duplex, due to the fact that the RV helix is held in place via nonspecific interactions with other polymerase in the crystal lattice. In case of PV EC structure, we only observe 2−4 base pairs of the downstream helix with sufficient density to allow for model building. The PV structure shows that the downstream helix is rotated by <180 degree such that the 5′ end of the helix is closer to the thumb domain than the fingers domain, whereas no such rotation is observed in case of RV. On the downstream template side, there is a conserved binding pocket for the $+2$ nucleotide and this anchoring interaction probably acts in concert with the upstream clamp to establish the high temporal stability of the ECs. The EC features an upstream RNA duplex that is pinched between the pinky finger and thumb domains such that the RNA exit channel is opened by nearly 4 Å as compared to the polymerase alone structures. Due to this tight grip on the exiting duplex between the finger and domain, a high temporal stability is observed and results in high processivity of the picornaviral ECs.

11.5.1.2.4 Translocation Step

After the formation of RdRP−RNA−NTP EC, the next step is the translocation of the polymerase by 1 base pair to position the next templating nucleotide in the active site for the next round of nucleotide addition. A number of crystal structures have also been solved in a post translocation state for various other viruses (Gong et al., 2013). However, no structures of translocation intermediates are currently

available for any RdRPs and the precise mechanism is not yet known. Once a stable polymerase–nucleic acid complex is formed, the polymerases can add thousands of nucleotides during elongation. High elongation processivity requires a stable association of template and primer in the polymerase, which prevents dissociation, but which should also be nonspecific and weak enough to facilitate the translocation movement upon each nucleotidyl transfer reaction step. For example, PV RdRP can add approximately 5000 nucleotides and 18,000 nucleotides in the absence and presence of its accessory protein 3AB, respectively, and can synthesize the entire genome in one single event (Rodriguez-Wells et al., 2001).

11.5.1.3 Termination

It is poorly understood how viral polymerases terminate nucleic acid synthesis at the 5′ end of the genome. Ending precisely at the 5′ terminus of the genome would be particularly challenging for viruses with linear genomes, such as single-stranded RNA or DNA viruses, and applied to HRV also since it is a single-stranded RNA virus.

11.5.2 Mechanism of VPg Uridylation by $3D^{pol}$

RNA virus uses different mechanisms to perform the critical task of RNA replication. In the case of HCV, NS5B contains a large thumb subdomain with a β-hairpin extension. Evidence suggests that the β-hairpin forms a scaffold upon which a 3′ terminal initiation complex can assemble. A similar de novo initiation mechanism has been proposed for the RdRP from bacteriophage φ6, but a different mechanism, primer dependent, is employed for PV, RHDV, and HRV in which a small viral peptide, VPg (also known as 3B), is supposed to play the role of a protein primer in the initiation of RNA synthesis. Actually, it is the uridylylated form of VPg which acts as a primer, so the process of uridylyation of Vpg has to be carried out and it is performed by 3D polymerase.

The covalent attachment of uridine monophosphate (UMP) to the hydroxyl group of a tyrosine residue located three residues away from the N-terminus of the small viral protein VPg is called the uridylyation of VPg. VPg, 3Dpol, poly (A), and UTP form a complex that allows transfer of UMP to the hydroxyl group of residue Y3 of VPg (Fig. 11.6). Although the exact molecular mechanism of VPg uridylyation by HRV 3D polymerase is not known, a few structural aspects are known by correlating with PV polymerase. Using the crystal structure of HRV16 3D polymerase, a front loading mechanism has been proposed for the uridylyation (Appleby et al., 2005). In the complex, the polymerase binds directly to VPg and utilizes a stem-loop cis-acting replication element

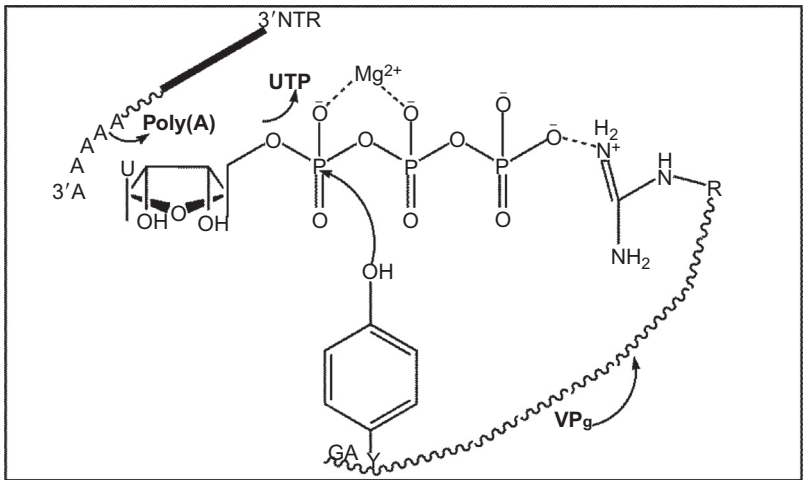

FIGURE 11.6 Uridylation of VPg by $3D^{Pol}$ to form VPg-pUpU which further acts as primer in the initiation step of RNA transcription. $3D^{pol}$ forms a complex with the 5′-terminal protein VPg and with the 3′-terminal end (3′ NTR) of the poly (A) tail of genome. The complementary nucleotide UTP is selected and positioned near the tyrosine of VPg, a process aided by R17 of VPg. $3D^{Pol}$ then catalyzes the formation of a phosphodiester bond between UMP and the hydroxyl group of tyrosine.

(CRE) as a template to uridylylate the tyrosine residue of VPg protein. This product, VPg-pU, is subsequently extended by at least one more uridine nucleotide to give VPg-pUpU. Residues: Gly376, Arg378, and Thr390 in HRV16 $3D^{Pol}$ map to the backside of the polymerase molecule at the junction between the palm and thumb subdomains and are believed to be essential for the efficient binding of 3AB (precursor of VPg) and uridylylation of VPg.

11.6 INHIBITORS OF RHINOVIRUS POLYMERASE

Currently, there are no licensed treatments or vaccines for RV infections, although several are in development. Pleconaril, a viral capsid inhibitor, has been shown to reduce the RV viral load in respiratory secretions and in shortening of the duration of respiratory symptoms in adults with RV respiratory tract infections (Pevear et al., 2005). But, it is not licensed for use in the United Kingdom and United States. Other medications that are under development for the treatment of RV infections include rupintrivir, vapendavir, OC459 (a CRTH2 receptor antagonist), and soluble ICAM-1. Due to an incomplete understanding of the

immune response to RVs and the large number of genetically distinct RV strains, the search for a suitable RV vaccine has so far proved difficult. Thus, studying the life cycle of the virus replication can help us in finding specific enzymes involved that could be targeted for drug designing.

The RV life cycle offers many opportunities for intervention. The initial stage of the viral life cycle involves binding to a cell surface receptor, endocytosis, acidification of the endosome, viral uncoating, and release of vRNA to the cytoplasm (Prchla et al., 1994). In the next stage, vRNA is translated as a single large polyprotein from an internal ribosomal entry site (IRES) which is located in the 5′ untranslated region of the RV genome. The polyprotein is then processed through sequential enzymatic cleavages by two virus-encoded proteinases, 2 A and 3 C proteinase (Foeger et al., 2003). Simultaneously, transcription of viral genome that is catalyzed by virus-encoded RNA polymerase begins. In the final stage of viral replication, RNA and capsid proteins are assembled into mature viral particles, which are then released by cell lysis. During the replication process, RNA viruses, including RV, modify the cellular functions to their advantage. For example, RV proteinase 2 A attacks the host translational machinery in susceptible HeLa cells by cleaving the eukaryotic initiation factor (eIF)-4GI and eIF4GII, thereby shutting off cap-dependent host cell protein synthesis (Glaser and Skern, 2000; Gradi et al., 2003). Drugs which interfere with any of the above steps would be beneficial in treating the RV infection. Here in our study, we focus on the compounds that inhibit the functioning of RNA polymerase enzyme.

11.6.1 Zinc

Hung and group investigated the effect of Zn^{2+} on the activity of HRV16 3D polymerase. Zn^{2+} was inhibitory at 60 mM when tested in the standard HRV16 3D assay buffer using PolyA/T as template. The IC_{50} values of Zn^{2+} tested against PolyA/T and sshRNA templates were reported. In the absence of DTT, Zn^{2+} has an IC_{50} of 0.6−1.7 mM when PolyA/T was used as template. With sshRNA, Zn^{2+} is sevenfold less inhibitory. The inhibition of RV 3D polymerase by zinc is not likely due to displacement of the catalytically essential Mg^{2+} ion, because the Mg^{2+} optimum concentration is at 1.5 mM, while the IC_{50} of Zn^{2+} is 12 μM (Hung et al., 2002). At this point, the mechanism of action by Zn^{2+} at the RNA polymerase enzyme is not known. But possible modes of action have been proposed by many authors for the in vitro inhibition of RV replication by Zn^{2+} where it inhibits the capsid polypeptides (Korant et al., 1974).

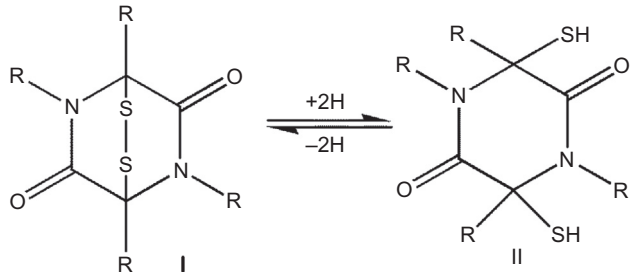

FIGURE 11.7 Structures of the oxidized (I) and the reduced (II) forms of epidithiapiperazinediones class of compounds. Gliotoxin is an important member of this class with antiviral activity.

11.6.2 Gliotoxin

Gliotoxin (Fig. 11.8A), a fungal metabolite, is an important member of the epidithiapiperazinediones class of compounds that inhibit the growth of several animal viruses, including picornaviruses. Earlier evidences indicated that it is a selective inhibitor of picornavirus RNA synthesis and had less effect on protein synthesis when added later during infection. The concentration of gliotoxin sufficient to block vRNA synthesis completely does not affect cellular RNA synthesis (Trown and Bilello, 1972).

The in vivo inhibitory effect of gliotoxin on HRV16 3D polymerase has an IC_{50} value of 150 μM (Hung et al., 2002). Kinetic experiments have also shown that the probable mode of action of this epidithiapiperazinedione is via the inhibition of viral RdRP rather than synthesis of this enzyme (Trown and Bilello, 1972). Previously, it has also been reported to inhibit the 3D polymerase of PV where it potently inhibited the incorporation of [^{3}H] uridine into PV RNA soon after its addition to the culture medium (Rodriguez and Carrasco, 1992).

In fact, two structural forms of gliotoxin exist, the oxidized (I) and the reduced form (II), but the inhibitory activity of gilotoxin is attributed to the oxidized form (I) (Fig. 11.7). This is because an interaction occurs between the inhibitor and protein via formation of a mixed disulfide between the disulfide bridge of the inhibitor and a sulfhydryl group on a protein (targeting the cysteine residue) and such an interaction is unlikely with the dithiol form (reduced form) of the inhibitor and hence the oxidized form is the active form.

11.6.3 Nucleoside and Nonnucleoside Analogs

The prospect of using nucleoside analogs in treating viral infections is a new frontier in designing novel antiviral therapy (Deval et al., 2014). Nucleoside analogs attack the active site of the polymerase and

need to be converted by the host cell machinery to the corresponding nucleotides, which can either be incorporated by the viral polymerase into the nascent RNA or induce premature termination of RNA synthesis (Carfi et al., 2007). 7-Deaza-2′-C-methyl-adenosine, a nucleoside molecule (Fig. 11.8B), displayed significant antiviral activity against

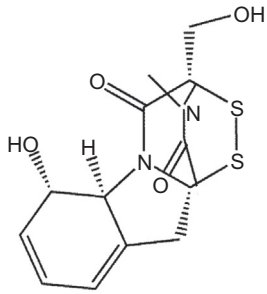

(A) **Gliotoxin**

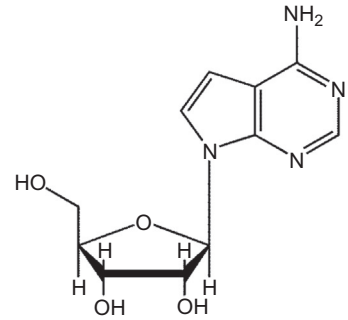

(B) **7-Deaza-2′-C-methyl-adenosine**

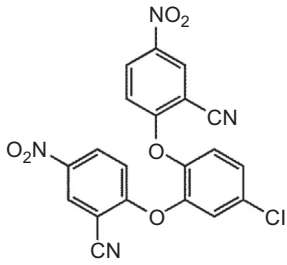

(C) **GPC-N114**

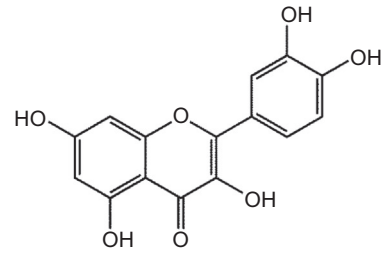

(D) **Quercetin**

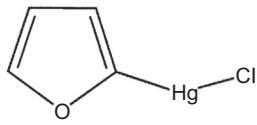

(E) **2-Furylmercury chloride**

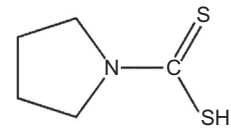

(F) **Pyrrolidine dithiocarbamate (PDTC)**

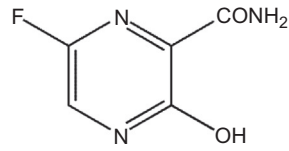

(G) **Favipiravir**

FIGURE 11.8 Structures of some inhibitors of rhinovirus $3D^{Pol}$.

positive-strand RNA viruses belonging to the *Flaviviridae* and *Picornaviridae* families. It showed in vivo activity against RV type 14 and 3 RNA polymerases (Olsen et al., 2004).

In contrast, non-nucleoside inhibitors (NNIs) are allosteric inhibitors believed to block the enzyme by preventing a conformational transition needed for the formation of a productive polymerase−RNA complex. Van der Linden and group reported an NNI, GPC-N114 (2,2′-[(4-chloro-1,2-phenylene)bis(oxy)]bis(5-nitro-benzonitrile)) (Fig. 11.8C) with broad-spectrum activity against enteroviruses and cardioviruses. The genus *Enterovirus* contains four human enterovirus species (HEV-A, -B, -C, -D), three HRV species (HRV-A, -B, -C), simian enterovirus, bovine enterovirus, and porcine enterovirus. All RVs included in the study (HRV14, HRV2) were found to be sensitive to the inhibitory effect of GPC-N114, with the EC_{50} values ranging from 0.1 μM to 1.7 μM. In vivo analysis showed that the inhibitor targeted the activity of RNA polymerase ($3D^{Pol}$). The analysis of the difference in the electron density maps revealed the presence of extra densities to position the inhibitor within a pocket located at the bottom of the template channel, mimicking the position of the template acceptor nucleotide, the nucleotide which will base pair with the incoming nucleotide. Hence, both the crystallographic studies as well as the order-of-addition experiment strongly suggest that the GPC-N114 affected the binding of the template−primer in the active site of $3D^{Pol}$ (Van Der Linden et al., 2015).

11.6.4 Quercetin

Quercetin (Fig. 11.8D), and its derivative 3-methylquercetin (Castrillo and Carrasco, 1987) were shown to inhibit the synthesis of PV RNA and this was attributed to the inhibition of vRNA polymerase $3D^{pol}$ (Neznanov et al., 2008). In the case of RV, Quercetin interferes with the processing of RV polyprotein by RV proteases and this process is required for activation of RNA polymerase ($3D^{Pol}$). Results demonstrated that quercetin significantly reduced both negative- and positive-strand vRNA and it is due to reduced cleavage of eIFG4II and reduction in viral capsid protein, VP2, suggesting that quercetin actually targets the initial polypeptide processing that in turn is required for both vRNA polymerase processing and for cleavage of eIFG4II. Another possibility could be that it may directly inhibit vRNA polymerase, thereby blocking genome translation and synthesis of new progeny virus (Ganesan et al., 2012).

11.6.5 2-Furylmercury Chloride (2-FMC)

The RdRP first copies input positive-strand RNA (viral genome) into negative-strand RNA, which, in turn, serves as a template for the

synthesis of viral progeny positive strands from a multistranded replicative intermediate (RI). The possible inhibitory effect of 2-FMC (Fig. 11.8E) in case of HRV2 serotype was examined by an in-house developed quantitative RV-specific RT-PCR ELISA method (Lauwers et al., 2001). The results showed that 2-FMC exerts its antiviral action by inhibiting the vRNA synthesis step during HRV2 replication in cells. Although the exact viral target protein is not known in this case, but it provides an opportunity to find the exact antiviral target of 2-FMC in the vRNA synthesis steps using escape mutants selected against 2-FMC (Verheyden et al., 2004).

11.6.6 Pyrrolidine Dithiocarbamate

Recently, pyrrolidine dithiocarbamate (PDTC) (Fig. 11.8F), has been described as a potent inhibitor of HRV multiplication. PDTC is effective against all tested HRV serotypes in several cell lines analyzed, without being toxic (Gaudernak et al., 2002). In a study performed by Krenn and coworkers, the data indicated that PDTC hampers the processing of the HRV polyprotein, thus targeting the enzyme viral proteases $2A^{Pro}$ and/or $3C^{Pro}$ (Krenn et al., 2005). PDTC also chelates various metal ions, leading to the formation of lipophilic dithiocarbamate−metal complexes (Thorn and Ludwig, 1962) and can thus promote cell entry of metals, e.g., diethyldithiocarbamate in the form of these lipophilic metal complexes. PDTC is found to increase the intracellular copper levels in thymocytes (Erl et al., 2000). Kim et al. (1999) demonstrated that PDTC can also increase the uptake of zinc ions, and it is known that zinc ion inhibits the activity of the $3D^{Pol}$ of HRV16 in vitro (Hung et al., 2002). Thus, it cannot be ruled out that apart from targeting protease enzyme, PDTC could also target the RNA polymerase enzyme ($3D^{Pol}$) function by increasing the intracellular zinc ion concentration (Krenn et al., 2005).

11.6.7 Favipiravir

Favipiravir (T-705; 6-fluoro-3-hydroxy-2-pyrazinecarboxamid, Fig. 11.8G) is an antiviral drug that selectively inhibited the RdRP of influenza virus. It showed specific activity against all three influenza A, B, and C (Furuta et al., 2013). It also inhibited the RV replication in HeLa cells, with an EC_{50} of 29 μg/mL (Furuta et al., 2002). Analysis showed that the primary mechanism of action of favipiravir against the influenza virus was specific inhibition of vRNA polymerase (Furuta et al., 2005). It is predicted that a similar mechanism might occur with other viruses, such as PV and RV, inhibited by favipiravir, which may

account for its broad-spectrum inhibition. Mechanistic studies show that the favipiravir and its form favipiravir-RMP (favipiravir-ribofuranosyl-50-monophosphate) do not inhibit influenza RNA polymerase activity, but it is the phosphoribosylated form, favipiravir-ribofuranosyl-50-triphosphate (RTP) that inhibits the enzyme. Metabolism of favipiravir to its triphosphate form occurs in an extracellular environment in a concentration-dependent manner. The vRNA polymerase mistakenly recognizes favipiravir-RTP as a purine nucleotide. This favipiravir-RTP is misincorporated in nascent vRNA, or it may act by binding to conserved polymerase domains, preventing incorporation of nucleotides for vRNA replication and transcription (Jin et al., 2013).

11.7 CONCLUSION

In this work we have given detailed recent studies on the structure, function, and inhibitors of the RV RNA polymerase. Crystal structures of the serotypes HRV1B, 14, and 16 have been recently determined. Not all serotypes have been studied extensively and an immense scope is still left for such crystallographic studies. RNA polymerase performs the dual function of RNA replication and uridylation of VPg. The mechanism of this uridylation process is still not fully understood. Also, various steps of replication processes are only modeled based on the PV and HIV-RT $3D^{Pol}$. Very little information is known about the termination step. These gaps need to be filled with further advancements using the techniques previously reported for other viruses of the *Picornaviridae* family. The more advance picture of the enzyme can help in bringing more specific antirhinoviral drugs. Currently no drug targeting the RV polymerase is approved to be clinically used to treat RV infection. Hence, drug design targeting this enzyme needs more attention of both experimental and theoretical chemists. Hopefully, this chapter may provide some guidelines in this direction.

References

Ackermann, M., Padmanabhan, R., 2001. De novo synthesis of RNA by the dengue virus RNA-dependent RNA polymerase exhibits temperature dependence at the initiation but not elongation phase. J. Biol. Chem. 276 (43), 39926–39937.

Ago, H., Adachi, T., Yoshida, A., Yamamoto, M., Habuka, N., Yatsunami, K., et al., 1999. Crystal structure of the RNA-dependent RNA polymerase of hepatitis C virus. Structure 7 (11), 1417–1426.

Andries, K., Dewindt, B., Snoeks, J., Wouters, L., Moereels, H., Lewi, P.J., et al., 1990. Two groups of rhinoviruses revealed by a panel of antiviral compounds present sequence divergence and differential pathogenicity. J. Virol. 64 (3), 1117–1123.

Appleby, T.C., Luecke, H., Shim, J.H., Wu, J.Z., Cheney, I.W., Zhong, W., et al., 2005. Crystal structure of complete rhinovirus RNA polymerase suggests front loading of protein primer. J. Virol. 79 (1), 277–288.
Arnold, J.J., Cameron, C.E., 1999. Poliovirus RNA-dependent RNA polymerase (3Dpol) is sufficient for template switching in vivo. J. Biol. Chem. 274, 2706–2716.
Arnold, J.J., Vignuzzi, M., Stone, J.K., Andino, R., Cameron, C.E., 2005. Remote site control of an active site fidelity checkpoint in a viral RNAdependent RNA polymerase. J. Biol. Chem. 280, 25706–25716.
Beckman, M.T., Kirkegaard, K., 1998. Site size of cooperative single-stranded RNA binding by poliovirus RNA-dependent RNA polymerase. J. Biol. Chem. 273 (12), 6724–6730.
Behrens, S.E., Tomei, L., De Francesco, R., 1996. Identification and properties of the RNA-dependent RNA polymerase of hepatitis C virus. EMBO J. 15, 12–22.
Biswal, B.K., Cherney, M.M., Wang, M., Chan, L., Yannopoulos, C.G., Bilimoria, D., et al., 2005. Crystal structures of the RNA-dependent RNA polymerase genotype 2a of hepatitis C virus reveal two conformations and suggest mechanisms of inhibition by non-nucleoside inhibitors. J. Biol. Chem. 280 (18), 18202–18210.
Carfi, M., Gennari, A., Malerba, I., Corsini, E., Pallardy, M., Pieters, R., et al., 2007. In vitro tests to evaluate immunotoxicity: a preliminary study. Toxicology 229 (1), 11–22.
Castrillo, J.L., Carrasco, L.U.I.S., 1987. Action of 3-methylquercetin on poliovirus RNA replication. J. Virol. 61 (10), 3319–3321.
Castro, C., Smidansky, E., Maksimchuk, K.R., Arnold, J.J., Korneeva, V.S., Götte, M., et al., 2007. Two proton transfers in the transition state for nucleotidyl transfer catalyzed by RNA- and DNAdependent RNA and DNA polymerases. Proc. Natl. Acad. Sci. USA 104, 4267–4272.
Castro, C., Smidansky, E.D., Arnold, J.J., Maksimchuk, K.R., Moustafa, I., Uchida, A., et al., 2009. Nucleic acid polymerases use a general acid for nucleotidyl transfer. Nat. Struct. Mol. Biol. 16, 212–218.
Choi, K.H., 2012. Viral polymerases. Viral Molecular Machines. Springer, Boston, MA, pp. 267–304.
Deval, J., Symons, J.A., Beigelman, L., 2014. Inhibition of viral RNA polymerases by nucleoside and nucleotide analogs: therapeutic applications against positive-strand RNA viruses beyond hepatitis C virus. Curr. Opin. Virol. 9, 1–7.
Erl, W., Weber, C., Hansson, G.K., 2000. Pyrrolidine dithiocarbamate induced apoptosis depends on cell type, density, and the presence of Cu^{2+} and Zn^{2+}. Am. J. Physiol. Cell Physiol. 278, 1116–1125.
Ferrer-Orta, C., Arias, A., Escarmís, C., Verdaguer, N., 2006. A comparison of viral RNA-dependent RNA polymerases. Curr. Opin. Struct. Biol. 16 (1), 27–34.
Foeger, N., Schmid, E.M., Skern, T., 2003. Human rhinovirus 2 2Apro recognition of eukaryotic initiation factor 4GI involvement of an exosite. J. Biol. Chem. 278 (35), 33200–33207.
Furuta, Y., Takahashi, K., Fukuda, Y., Kuno, M., Kamiyama, T., Kozaki, K., et al., 2002. In vitro and in vivo activities of anti-influenza virus compound T-705. Antimicrob. Agents Chemother. 46 (4), 977–981.
Furuta, Y., Takahashi, K., Kuno-Maekawa, M., Sangawa, H., Uehara, S., Kozaki, K., et al., 2005. Mechanism of action of T-705 against influenza virus. Antimicrob. Agents Chemother. 49 (3), 981–986.
Furuta, Y., Gowen, B.B., Takahashi, K., Shiraki, K., Smee, D.F., Barnard, D.L., 2013. Favipiravir (T-705), a novel viral RNA polymerase inhibitor. Antiviral Res. 100 (2), 446–454.
Ganesan, S., Faris, A.N., Comstock, A.T., Wang, Q., Nanua, S., Hershenson, M.B., et al., 2012. Quercetin inhibits rhinovirus replication in vitro and in vivo. Antiviral Res. 94 (3), 258–271.

Garriga, D., Ferrer-Orta, C., Querol-Audí, J., Oliva, B., Verdaguer, N., 2013. Role of motif B loop in allosteric regulation of RNA-dependent RNA polymerization activity. J. Mol. Biol. 425 (13), 2279–2287.
Gaudernak, E., Seipelt, J., Triendl, A., Grassauer, A., Kuechler, E., 2002. Antiviral effects of pyrrolidine dithiocarbamate on human rhinoviruses. J. Virol. 76, 6004–6015.
Gerber, K., Wimmer, E., Paul, A.V., 2001. Biochemical and genetic studies of the initiation of human rhinovirus 2 RNA replication: purification and enzymatic analysis of the RNA-dependent RNA polymerase 3Dpol. J. Virol. 75 (22), 10969–10978.
Glaser, W., Skern, T., 2000. Extremely efficient cleavage of eIF4G by picornaviral proteinases L and 2A in vitro. FEBS lett. 480 (2–3), 151–155.
Gnadig, N.F., Beaucourt, S., Campagnola, G., Borderia, A.V., Sanz-Ramos, M., Gong, P., et al., 2012. Coxsackievirus B3 mutator strains are attenuated in vivo. Proc. Natl Acad. Sci. USA 109, E2294–E2303.
Gong, P., Peersen, O.B., 2010. Structural basis for active site closure by the poliovirus RNA-dependent RNA polymerase. Proc. Natl. Acad. Sci. 107, 22505–22510.
Gong, P., Kortus, M.G., Nix, J.C., Davis, R.E., Peersen, O.B., 2013. Structures of coxsackievirus, rhinovirus, and poliovirus polymerase elongation complexes solved by engineering RNA mediated crystal contacts. PLOS One 8 (5), e60272.
Gradi, A., Svitkin, Y.V., Sommergruber, W., Imataka, H., Morino, S., Skern, T., et al., 2003. Human rhinovirus 2A proteinase cleavage sites in eukaryotic initiation factors (eIF) 4GI and eIF4GII are different. J. Virol. 77 (8), 5026–5029.
Greve, J.M., Davis, G., Meyer, A.M., Forte, C.P., Yost, S.C., Marlor, C.W., et al., 1989. The major human rhinovirus receptor is ICAM-1. Cell 56 (5), 839–847.
Hansen, J.L., Long, A.M., Schultz, S.C., 1997. Structure of the RNA-dependent RNA polymerase of poliovirus. Structure 5 (8), 1109–1122.
Hofer, F., Gruenberger, M., Kowalski, H., Machat, H., Huettinger, M., Kuechler, E., et al., 1994. Members of the low density lipoprotein receptor family mediate cell entry of a minor-group common cold virus. Proc. Natl. Acad. Sci. USA 91, 1839–1842.
Huang, H., Chopra, R., Verdine, G.L., Harrison, S.C., 1998. Structure of a covalently trapped catalytic complex of HIV-1 reverse transcriptase: implications for drug resistance. Science 282, 1669–1675.
Hung, M., Gibbs, C.S., Tsiang, M., 2002. Biochemical characterization of rhinovirus RNA-dependent RNA polymerase. Antiviral Res. 56 (2), 99–114.
Jacobo-Molina, A., Ding, J., Nanni, R.J., Clark Jr., A.D., Lu, X., et al., 1993. Crystal structure of human immunodeficiency virus type 1 reverse transcriptase complexed with double-stranded DNA at 3.0 Å resolution shows bent DNA. Proc. Natl. Acad. Sci. USA 90, 6320–6324.
Jin, Z., Smith, L.K., Rajwanshi, V.K., Kim, B., Deval, J., 2013. The ambiguous basepairing and high substrate efficiency of T-705 (favipiravir) ribofuranosyl 50- triphosphate towards influenza A virus polymerase. PLOS One 8, e68347.
Kim, C.H., Kim, J.H., Xu, J., Hsu, C.Y., Ahn, Y.S., 1999. Pyrrolidine dithiocarbamate induces bovine cerebral endothelial cell death by increasing the intracellular zinc level. J. Neurochem. 72, 1586–1592.
Kim, M.J., Zhong, W., Hong, Z., Kao, C.C., 2000. Template nucleotide moieties required for de novo initiation of RNA synthesis by a recombinant viral RNA-dependent RNA polymerase. J. Virol. 74 (22), 10312–10322.
Kim, W.K., Gern, J.E., 2012. Updates in the relationship between human rhinovirus and asthma. Allergy Asthma Immunol. Res. 4 (3), 116–121.
Korant, B.D., Kauer, J.C., Butterworth, B.E., 1974. Zinc ions inhibit replication of rhinoviruses. Nature 248, 588–590.
Krenn, B.M., Holzer, B., Gaudernak, E., Triendl, A., Van Kuppeveld, F.J., Seipelt, J., 2005. Inhibition of polyprotein processing and RNA replication of human rhinovirus by pyrrolidine dithiocarbamate involves metal ions. J. Virol. 79 (22), 13892–13899.

Lamson, D., Renwick, N., Kapoor, V., Liu, Z., Palacios, G., Ju, J., et al., 2006. MassTag polymerase-chain-reaction detection of respiratory pathogens, including a new rhinovirus genotype that caused influenza-like illness in New York State during 2004–2005. J. Infect. Dis. 194, 1398–1402.

Lauwers, S., Vander Heyden, Y., Rombaut, B., 2001. Screening of an enterovirus specific RT-PCR ELISA method for the quantification of enterovirus genomes in human body fluids by means of a three-level experimental design. J. Pharm. Biomed. Anal. 25 (1), 131–142.

Lesburg, C.A., Cable, M.B., Ferrari, E., Hong, Z., Mannarino, A.F., Weber, P.C., 1999. Crystal structure of the RNA-dependent RNA polymerase from hepatitis C virus reveals a fully encircled active site. Nat. Struct. Mol. Biol. 6 (10), 937–943.

Love, R.A., Maegley, K.A., Yu, X., Ferre, R.A., Lingardo, L.K., Diehl, W., et al., 2004. The crystal structure of the RNA-dependent RNA polymerase from human rhinovirus: a dual function target for common cold antiviral therapy. Structure 12 (8), 1533–1544.

Monto, A.S., Cavallaro, J.J., 1971. The Tecumseh study of respiratory illness. II. Patterns of occurrence of infection with respiratory pathogensm 1965–1969. Am. J. Epidemiol. 94, 280–289.

Morrow, C.D., Lubinski, J.O.H.N., Hocko, J.A.N.E.T., Gibbons, G.F., Dasgupta, A.S.I.M., 1985. Purification of a soluble template-dependent rhinovirus RNA polymerase and its dependence on a host cell protein for viral RNA synthesis. J. Virol. 53 (1), 266–272.

Moustafa, I.M., Shen, H., Morton, B., Colina, C.M., Cameron, C.E., 2011. Molecular dynamics simulations of viral RNA polymerases link conserved and correlated motions of functional elements to fidelity. J. Mol. Biol. 410, 159–181.

Neznanov, N., Kondratova, A., Chumakov, K.M., Neznanova, L., Kondratov, R., Banerjee, A.K., et al., 2008. Quercetinase pirin makes poliovirus replication resistant to flavonoid Quercetin. DNA Cell Biol. 27 (4), 191–198.

Ng, K.K., Cherney, M.M., Vázquez, A.L., Machí;n, Á., Alonso, J.M.M., Parra, F., et al., 2002. Crystal structures of active and inactive conformations of a caliciviral RNA-dependent RNA polymerase. J. Biol. Chem. 277 (2), 1381–1387.

Olsen, D.B., Eldrup, A.B., Bartholomew, L., Bhat, B., Bosserman, M.R., Ceccacci, A., et al., 2004. A 7-deaza-adenosine analog is a potent and selective inhibitor of hepatitis C virus replication with excellent pharmacokinetic properties. Antimicrob. Agents Chemother. 48 (10), 3944–3953.

Pathak, H.B., Ghosh, S.K., Roberts, A.W., Sharma, S.D., Yoder, J.D., Arnold, J.J., et al., 2002. Structure-function relationships of the RNA-dependent RNA polymerase from poliovirus ($3D^{pol}$). A surface of the primary oligomerization domain functions in capsid precursor processing and VPg uridylylation. J. Biol. Chem. 277, 31551–31562.

Paul, A., 2002. Possible Unifying Mechanism of Picornavirus Genome Replication. In: Semler, B., Wimmer, E. (Eds.), Molecular Biology of Picornavirus. ASM Press, Washington, DC, pp. 227–246. Available from: https://doi.org/10.1128/9781555817916, ch19.

Pevear, D.C., Hayden, F.G., Demenczuk, T.M., Barone, L.R., Mckinlay, M.A., Collett, M.S., 2005. Relationship of Pleconaril susceptibility and clinical outcomes in treatment of common colds caused by Rhinoviruses relationship of Pleconaril susceptibility and clinical outcomes in treatment of common colds caused by Rhinoviruses. Antimicrob. Agents Chemother. 49 (11), 4492–4499.

Pfeiffer, J.K., Kirkegaard, K., 2005. Increased fidelity reduces poliovirus fitness and virulence under selective pressure in mice. PLOS Pathog 1 (2), e11.

Pitkaranta, A., Hayden, F.G., 1998. Rhinoviruses: important respiratory pathogens. Ann. Med. 30, 529–537.

Prchla, E., Kuechler, E., Blaas, D., Fuchs, R., 1994. Uncoating of human rhinovirus serotype 2 from late endosomes. J. Virol. 68 (6), 3713–3723.

Quadt, R., Kao, C.C., Browning, K.S., Hershberger, R.P., Ahlquist, P., 1993. Characterization of a host protein associated with brome mosaic virus RNA-dependent RNA polymerase. Proc. Natl. Acad. Sci. USA 90 (4), 1498–1502.

Rodriguez, P.L., Carrasco, L.U.I.S., 1992. Gliotoxin: inhibitor of poliovirus RNA synthesis that blocks the viral RNA polymerase 3Dpol. J. Virol. 66 (4), 1971–1976.

Rodriguez-Wells, V., Plotch, S.J., DeStefano, J.J., 2001. Primer-dependent synthesis by poliovirus RNA-dependent RNA polymerase (3Dpol). Nucleic Acids Res. 29 (13), 2715–2724.

Steitz, T.A., 1998. A mechanism for all polymerases. Nature 391, 231–232.

Thorn, G.D., Ludwig, R.A., 1962. The Dithiocarbamates and Related Compounds. Elsevier Publishing Co, Amsterdam, New York.

Tomassini, J.E., Colonno, R.J., 1986. Isolation of a receptor protein involved in attachment of human rhinoviruses. J. Virol. 58, 290–295.

Trown, P.W., Bilello, J.A., 1972. Mechanism of action of gliotoxin: elimination of activity by sulphydryl compounds. Antimicrob. Agents Chemother. 2, 261–266.

Van Der Linden, L., Vives-Adrián, L., Selisko, B., Ferrer-Orta, C., Liu, X., Lanke, K., et al., 2015. The RNA template channel of the RNA-dependent RNA polymerase as a target for development of antiviral therapy of multiple genera within a virus family. PLOS Pathog. 11 (3), e1004733.

Verheyden, B., Andries, K., Rombaut, B., 2004. Mode of action of 2-furylmercury chloride, an anti-rhinovirus compound. Antiviral Res. 61 (3), 189–194.

Vignuzzi, M., Wendt, E., Andino, R., 2008. Engineering attenuated virus vaccines by controlling replication fidelity. Nat. Med. 14, 154–161.

Xiang, W., Paul, A.V., Wimmer, E., 1997. RNA signals in entero- and rhinovirus genome replication. Semin. Virol. 8, 256–273.

Yang, X., Smidansky, E.D., Maksimchuk, K.R., Lum, D., Welch, J.L., Arnold, J.J., et al., 2012. Motif D of viral RNA-dependent RNA polymerases determines efficiency and fidelity of nucleotide addition. Structure 20 (9), 1519–1527.

Yoshinari, S., Nagy, P.D., Simon, A.E., Dreher, T.W., 2000. CCA initiation boxes without unique promoter elements support in vitro transcription by three viral RNA-dependent. RNA polymerases. RNA 6 (5), 698–707.